

A Strong Shock Wave Structure in Low Density Gas Mixture Flow Past a Cylinder

Mikhail Yu. Plotnikov, Alexei K. Rebrov

Institute of Thermophysics

1, Lavrentieva av., 630090, Novosibirsk, Russia

E-mail: plotnikov@itp.nsc.ru, rebrov@itp.nsc.ru

The hypersonic flow of a binary mixture flow of gases (with disparate molecular masses) around a cylinder is investigated using the direct simulation Monte Carlo method over a wide range of rarefaction: from the Knudsen number $Kn = 0.01$ to a free molecular flow. The effect of a mixture composition on the region of essential nonequilibrium near the cylinder and the heat flow is studied.

Keywords: hypersonic rarefied gas flow, cylinder, heat transfer, nonequilibrium, mixture.

PACS: 47.45-n

The study of hypersonic rarefied gas flow around a cylinder attracted attention of researchers from the middle of the last century [1, 2]. In recent years the development of numerical methods, on the one hand, and permanent extension of computational possibilities, on the other, has opened ways to solution of complicated problems in this field. Usually the uniform gas flows were considered. In [3] the influence of vibrational relaxation and chemical reactions on the structure of the shock-wave front for a cylindrical body descending in the Martian atmosphere was studied for small Knudsen numbers. In [4, 5] the nonequilibrium zone for the transversal hypersonic flow of a mixture of monoatomic gases over infinite strip and a cylinder was considered. In the presented work, the main interest is focused on study of the influence of the molecular energy exchange on the flow field and heat transfer for nonequilibrium hypersonic flow over a cylinder (for binary gas mixtures).

The Problem Statement and its Solution by Direct Simulation Monte Carlo Method

The gas flow around a cylinder with the diameter d and the infinite length is considered. The axis of the cylinder is perpendicular to the flow direction. The orthogonal co-ordinate system (X, Y, Z) is used: axis X is directed along the flow, axis Z coincides with the axis of cylinder. It was supposed that a planar undisturbed flow source is located in a section $x=x_s < 0$. The origin of the co-ordinates coincides with the axis of the cylinder, and the gas is fully absorbed downstream in the section $x=x_e$.

In view of symmetry of this problem, the plane $y=0$ is assumed to be mirror-like. The boundary conditions on the planes $y=y_e$ correspond to the undisturbed flow. Particles back scattered to the source surface are absorbed. On the source surface, the translational temperature is T_s , velocity is V_s and the number density is n_s . The surface temperature of the cylinder is constant and equal to T_w .

The attention was paid to peculiarities of a stationary flow of a gaseous mixture with strongly disparate molecular masses. In previous paper [5] the binary gas flow past a cylinder was studied; the mixture was a composition of xenon and helium with atomic mass ratio 32.78. In this paper we consider two variants of mixtures: 1) $He+Xe$; 2) He + heavy diatomic gas having collisional parameters and mass of Xe . Let us choose the name \tilde{Xe} belongs to the heavy diatomic gas.

The interaction of particles was described by the VSS molecular model [6]. The internal degrees of freedom for particles are considered with the Borgnakke-Larsen model [6]. The reflection of atoms of helium from the cylinder

surface was assumed to be of diffusive type. The heavy component with probability α is absorbed by the surface and with probability $(1-\alpha)$ undergoes the diffusive reflection.

The thermodynamic equilibrium was taken for the undisturbed flow. That means the equality between temperatures of the components and temperatures for all degrees of freedom. The mixture composition is determined by the number density ratio $\Theta = 100n_S^X / n_S^H$. The superscripts X and H denote the heavy and light molecules, correspondingly.

To reduce the problem to a dimensionless form, the temperature T_S , density n_S^H , the most probable molecular thermal speed at temperature T_S , and the molecular mean free path L were used as the reference values. The value L was determined only by parameters of helium in the undisturbed flow. Eventually the problem is determined by the following parameters: the Mach number M_S^H , the temperature factor T_w/T_S , the concentration Θ , the Knudsen number $Kn=L/d$, the probability of heavy particle sorption α , the number of internal degrees of freedom of the heavy component, and the relaxation collision number for internal energy Z_R .

The analysis of the computational domain has allowed us to find the location of the boundary planes $x=x_e$ and $y=y_e$, where the flow around the cylinder is free from boundary influence.

For each component of the mixture, the following parameters were computed: density, the Mach number, temperatures in three directions (along flow T_x , perpendicular to flow T_y , and T_z), average translational temperature $T = (T_x + T_y + T_z)/3$, rotational temperature, and the gas-to-cylinder heat flux.

The computational experiments have shown that the accuracy of determination of heat flux strongly depends on the cell width and the time step, and, certainly, on the number of simulated particles. It was enough to use from 1 million to 2.5 million particles. The stationary solution was the result of a large number of repetitions. The accuracy of calculations was monitored by variation of the cell widths and time steps.

Results of Computational Experiments

Computational experiments were performed for the following range of parameters: $Kn = 0.01 \div \infty$; $\Theta = 1$ and 10 ; $\alpha = 0 \div 1$, $T_w/T_S = 9.33$. The velocity range for the incident flow was chosen as corresponding to the Mach number (for helium) equal to 5. The Mach number for the monatomic gas mixture in the undisturbed flow (for the considered concentrations) equals 5.73 and 9.86, correspondingly. In several cases it is convenient to present data through the temperature normalized to the stagnation temperature T_0 . For the Mach number $M_S = 5.0$, the stagnation temperature is $T_0 = 9.33T_S$ (for monoatomic gas flow). The important parameter of this problem is the recovery temperature T_r . For the considered the Mach number and for free-molecular flow of monoatomic gas, the recovery temperature is $T_r = 11.66T_S$ [2].

The main interest of this work is the study of nonequilibrium processes and their influence on transfer processes. The region of the disturbed flow mostly depends on the Knudsen number, the mixture composition, and probability of heavy particle sorption on the surface of the cylinder. The typical pattern of hypersonic rarefied flow in pure *He* across the cylinder has several features [5, fig. 1]. The temperature anisotropy is announced via translational nonequilibrium near the cylinder. The behavior of parameters at $Kn=5$ is close to the free-molecular flow. At $Kn \sim 0.1$ the pronounced maximum in the behavior of T_x upstream of the cylinder indicates the usual shock wave formation. At Knudsen number $Kn \leq 0.1$, the flow can generate a well-defined reflected shock wave.

Introduction of heavy component into helium flow causes a qualitative change in the parameter distributions in the flow - all due to the inertia mechanism of gas separation and lag of collisional relaxation. It is obvious from fig. 1, where the parameter distributions are plotted along the symmetry axis ahead the cylinder for the cases of helium flow (a, b) and \tilde{X}_e flow (c, d) for the Knudsen number 0.1 (a,c) and 5 (b,d), for the heavy component concentration $\Theta=10$. For $Kn=0.1$, the shock layer ahead the cylinder demonstrates a high-temperature zone with a high nonequilibrium degree (this is different from the case of pure gas [5, 7]). The parameter distributions are evidence about a merging of the shock wave with the compression layer. Difference in the extent of nonequilibrium zone for the heavy and light components is caused by the spatial inertia-driven separation of gases.

In general, these nonequilibrium features are typical for the flow with the Knudsen number equal to 5 (the only difference is complete elimination of gas-dynamically compressed layer in the shock-wave layer). The cylinder is in the zone of almost free-molecular flow. The significant changes occur at distance of 2-3 L .

Another direction for study of shock layer structure was comparison of behavior for mixtures *He+Xe* and *He+ \tilde{X}_e* for small Knudsen numbers. Fig. 2a shows the distribution of macroparameters of *He* in a mixture *He+Xe* and *He+ \tilde{X}_e* at the concentration of heavy component $\Theta=10$ (with total reflection). The thin curves show the data for

helium in a mixture $He+Xe$, thick lines, for mixture $He+\tilde{Xe}$. One can notice that there is no strong effect of the internal energy of gas \tilde{Xe} on parameters distribution along the symmetry axis ahead the cylinder. Fig. 2b is a plotting for gases Xe and \tilde{Xe} in a mixture $He+Xe$ and $He+\tilde{Xe}$. One can see a typical nonequilibrium at the shock wave front.

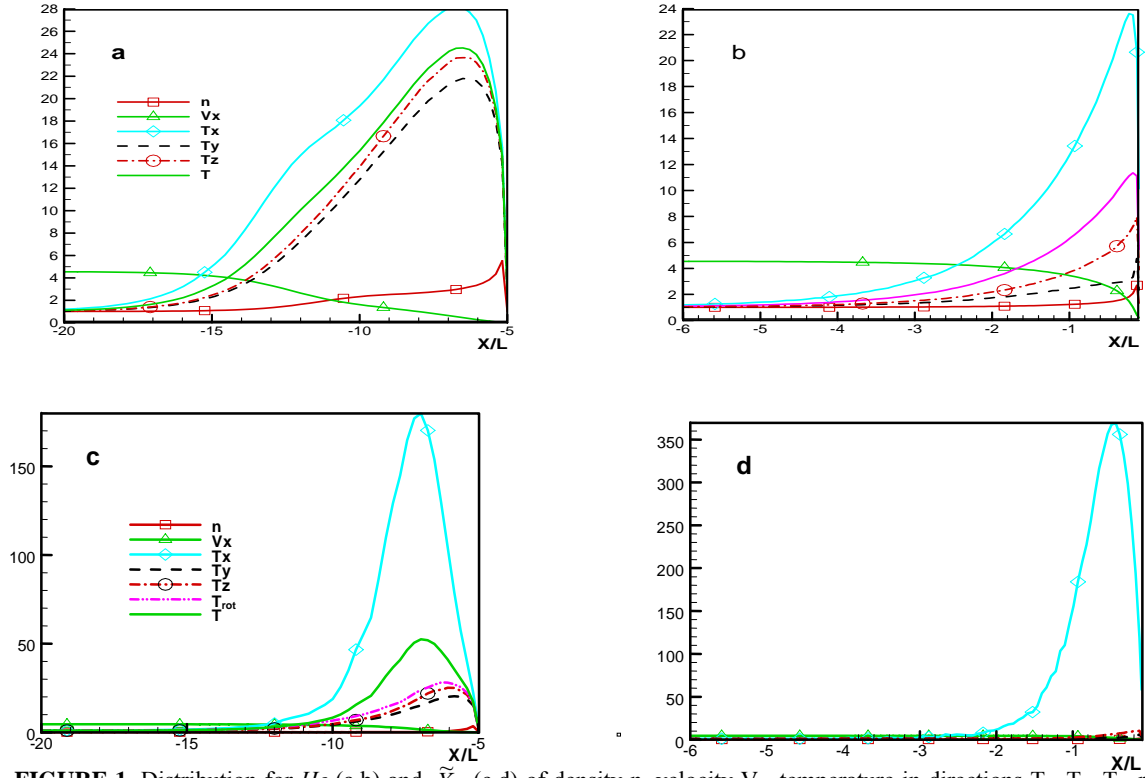


FIGURE 1. Distribution for He (a,b) and \tilde{Xe} (c,d) of density n , velocity V_x , temperature in directions T_x , T_y , T_z , rotational temperature T_{rot} and average temperature T along the plane of symmetry for $Kn = 0.1$ (left) and $Kn=5$ (right) for the flow of gas mixture $\Theta=10$.

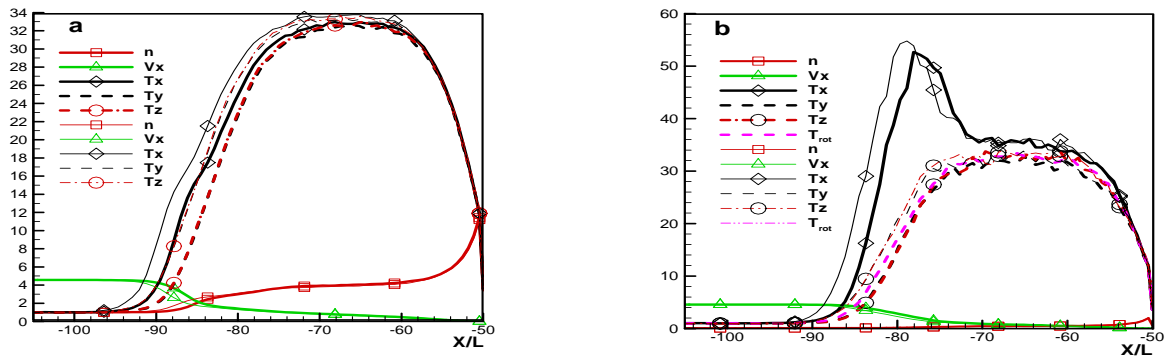


FIGURE 2. Distribution for He (a), Xe and \tilde{Xe} (b) of density n , velocity V_x , temperature in directions T_x , T_y , T_z , and rotational temperature T_{rot} along the plane of symmetry for $Kn = 0.01$, for the flow of gas mixture $\Theta=10$. The thick lines show the data for mixture $He+Xe$. The thin lines show the data for mixture $He+\tilde{Xe}$.

The flow exhibits several features of disturbed layer around the cylinder revealed in computational experiments:

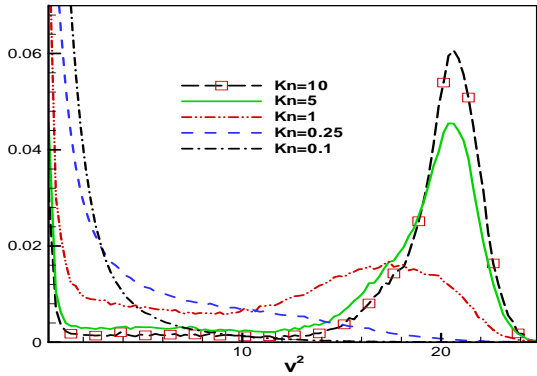
1) for Knudsen number $Kn \leq 0.1$, the pure helium flow can generate a reflected shock wave. At $\Theta=1$ we see a similar pattern for helium flow. But at $\Theta=10$ the shock wave is “smeared” and at the Knudsen number equal to 0.01, the helium shock wave exhibits unusual structure - without peak of the longitudinal temperature. The compressed layer shows superposition of the shock compression and heat transfer.

2) heavy particles for $\Theta=1$ have a small impact on the helium flow; this influence becomes still smaller with increase of Knudsen numbers.

3) the extent of the disturbed flow for a mixture is longer than for pure helium; for heavy atoms this zone is shorter than for helium.

The search experiments on study of influence of rotational degrees of freedom on the structure and macro-parameters of the flow revealed several interesting results. In particular, in modeling of $He + \tilde{X}e$ flow around a cylinder the number of collisions Z_R for relaxation of rotational energy was varied. The increase by order (from 1 to 10) brings minor changes in calculated macroparameters (except of rotational temperature). That is why we accepted this number equal to 1 in most of our computations.

The interaction of gas flow with the surface is considered below. Particularly the energy spectrum for the heavy



particle colliding the surface is presented. The qualitative presentation about the translational energy of heavy particles bombarding the cylinder surface for the concentration $\Theta=10$ is given in fig.3. The distribution function of the square of velocity of heavy particles that interact with the cylinder at the range of Knudsen number from 0.1 to 10 at complete reflection is plotted. One can observe a transition of particle energy from almost single-mode distribution for $Kn=10$ to the bimodal distribution for $Kn=1$ and then back to single-mode distribution for $Kn=0.1$ with a peak at zero velocity. As it was expected, for $\alpha=1$ there is no bimodal distribution for xenon atom energy.

FIGURE 3. Distribution functions of the square of velocity (V^2) of Xe colliding with the cylinder for different Knudsen numbers. $\Theta=10$, $\alpha=0$.

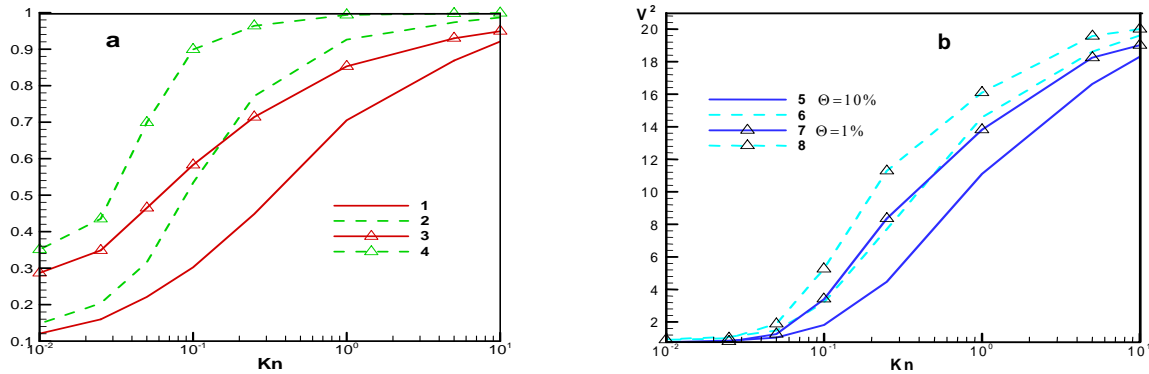


FIGURE 4. a. The ratio (for $\tilde{X}e$) of the number of particles experiencing the first collision with the surface to the total number of collisions with the surface (curve 1 for $\Theta=10$ and 3 for $\Theta=1$). The ratio (for $\tilde{X}e$) of the kinetic energies of particles experiencing the first collision with the surface to the total kinetic energies of particles that interact with the surface (curve 2 for $\Theta=10$ and 4 for $\Theta=1$). b. Dependency of the square of velocity for $\tilde{X}e$ on the Knudsen number at $\alpha=0$. The curves 7 and 8 correspond to the case $\Theta=1$, curves 5, 6- $\Theta=10$. (6, 8) - data for particles experiencing the first collision with surface and (5, 7) - for all particles collided.

The detail information about the energy of particles reaching the surface is of interest for choosing the optimal modes of thin film deposition. The DSMC allows us to track down the history of the particle motion. It is quite interesting to estimate the role of particles undergoing more than one collision with the cylinder surface. We considered only the particles $\tilde{X}e$ that hit the windward side of the cylinder ($x < 0$). Fig. 4a present the ratio of the

number of particles experiencing the first collision with the surface to the total number of collisions with the surface (curves 1 for $\Theta=10$ and 3 for $\Theta=1$). We also plotted the ratio of kinetic energies of particles experiencing the first collision with the surface to the total kinetic energies of particles that interact with the surface (curves 2 and 4). One can see that for $Kn > 1$ the role of particles reflected from the target is insignificant. For $Kn < 0.1$ the reflected particles produce a “cushion” around the cylinder, so the probability of the surface heating with particles from the undisturbed flow is reduced greatly. Note also that this “outer” particle will collide (with a high probability) in the shock layer, with a considerable change of the particle energy.

Fig. 4b presents the data for the square of the velocity of \tilde{X}_e for the case of total reflection. The curves 7 and 8 correspond to the case $\Theta=1$. Curves 5 and 6 correspond to the case $\Theta=10$. Data is calculated for the case of the first-collision particles and for all collided particles. We observe a drastic decrease in the particle kinetic energy with the Knudsen number. For the “fresh” collided molecules this decrease emphasizes the role of relaxation processes in the compressed layer. The curves for a mixture with $\Theta=1$ are above the mixture with $\Theta=10$. This can be explained by retarding of heavy particles on the reflected ones.

FIGURE 5. Dependency of the square of velocity of particles He and \tilde{X}_e that hit the windward part of the cylinder on the Knudsen number. $\Theta=10$. Curves without symbols correspond to $\alpha=0$, with symbols, $\alpha=1$. Also dependency for the rotational energy of particles \tilde{X}_e on the Knudsen number is presented.

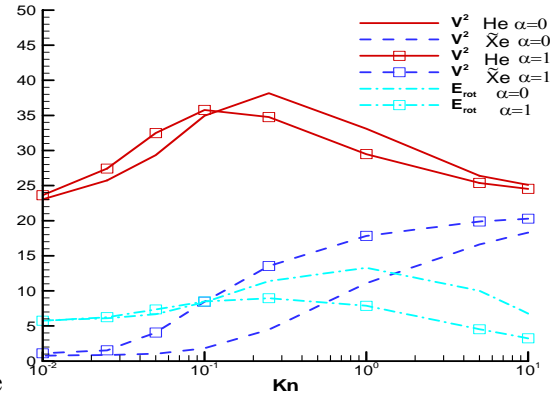


Fig. 5 is the plot of the square of velocity for particles He and \tilde{X}_e that hit the windward side of the cylinder. The data is plotted for $\Theta=10$. For heavy particles (\tilde{X}_e) we observe a quite expected monotonic decrease of the square of velocity with decreasing Kn . For the case $\alpha=0$ the decline rate is stronger due to diffusive reflection of heavy particles. For He one can see a distinct maximum around Knudsen numbers 0.1 ($\alpha=1$) and 0.25 ($\alpha=0$). This non-monotonous behavior is explained by acceleration of He with heavy particles as the Knudsen number increases up to $Kn \sim 0.1$. With the further growth of Kn , the slipping becomes stronger and the velocity of He decreases. Also on this figure dependency for the rotational energy of particles \tilde{X}_e on the Knudsen number is presented for $\alpha=0$ and $\alpha=1$. These graphs rather reflect the state of thermal motion energy in the mixture, i.e. existence of the temperature maximum in the compressed layer. The important result of this simulation is the established fact that for $Kn < 0.1$ we have a compressed layer which is enough for deceleration of heavy particles before hitting the surface.

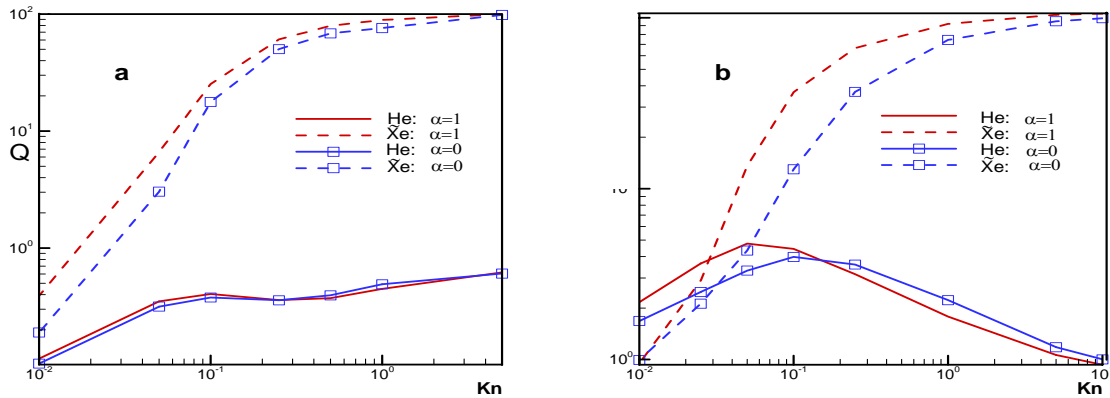


FIGURE 6. Dependency of the heat flux for $He + \tilde{X}_e$ mixture for the cases of total reflection ($\alpha=1$) and total sorption ($\alpha=0$) for the heavy component. a - $\Theta=1$, b - $\Theta=10$.

Fig. 6 present data on the surface-integrated heat flux to the cylinder as a function of the Knudsen number for mixture $He + \tilde{X}_e$ (for the heavy component cases of total reflection ($\alpha=1$) and total sorption ($\alpha=0$) are considered). The behavior of heat fluxes is qualitatively similar to the known laws for pure gases [7]. The curves of heat fluxes for mixture $He + Xe$ are coincided with the curves of heat fluxes for mixture $He + \tilde{X}_e$ (with an accuracy of

several percents). For $\Theta = 1$ (Fig. 6a) the heat flux for heavy component differ from helium heat flux for $Kn > 0.05$ by more then one order. For $\Theta = 10$ (Fig. 6b) the heat flux from the heavy component (at low Knudsen numbers) is lower than one for the mixture with $\Theta = 1$. The heat flux from helium at $\Theta = 10$ has a maximum near the Knudsen number 0.05 ($\alpha = 1$) and 0.1 ($\alpha = 0$), which is in agreement with the trend for helium atom kinetic energy (Fig. 5). The shift of peaks to the lower Knudsen numbers is explained by the fact that data in Fig. 5 takes into account only particles hitting the windward side of the cylinder.

Conclusion

Within the structure of shock waves and compressed layers generated in flow of gases with disparate molecular masses, several important features of hypersonic flow past a cylinder appear due to a lag in translational and rotational relaxation of the heavy component at interaction with the light component:

1) about flow pattern:

a) the admixture of the heavy component with concentration $\Theta = 1$ practically does not change the structure of the shock layer of helium flow;

b) at the Knudsen number ~ 0.1 , the shock layer is a superposition of a shock wave and a compression layer;

c) at the Knudsen number ~ 0.01 and concentration $\Theta = 10$, a typical nonequilibrium “viscous” layer of the shock wave is observed for the heavy component only;

2) about the molecule energies:

a) for the case of complete reflection at $Kn < 0.1$, a dense cloud of molecules is created that prevents the collisionless access of heavy molecules (from the undisturbed stream) to the cylinder;

b) at $Kn < 0.1$ the acceleration of heavy molecules is retarded and the conditions become close to those for streamlining with an equilibrium flow;

3) about heat flux:

a) the heat flux for the heavy component at numbers $Kn > 1$ exceeds the heat flux from He almost by two orders;

b) at $\Theta = 1$ the heat flux from the heavy component is higher than for the light component at $Kn \geq 0.01$;

c) at concentration $\Theta = 10$ the heat fluxes from the heavy and light components are almost equal at $Kn \sim 0.03 - 0.04$.

ACKNOWLEDGMENTS

The work was supported by the RFBR (grant N 06-01-00292), integration grant of Presidium RAS (8.11) and by grant for support of the Leading Scientific Schools (N 02.445.11.7293).

REFERENCES

1. Kogan M.N., Rarefied Gas Dynamics, Plenum Publ. Co., New York, 1969.
2. Koshmarov Yu. A., Ryjov Yu. A., Applied Dynamics of Rarefied Gas, Moscow, 1977. (in Russian)
3. Ivanov M.S., Bondar Ye.A., Markelov G.N., Gimelshein S.F., and Taran J.P., Study of the Shock Wave Structure about a Body Entering the Martian Atmosphere, in Proc. of 23 Intern. Symp. on RGD, edited by A.D. Ketsdever and E.P. Muntz. Melville, N.Y.: AIAA. 2003. V. 663. pp.481-488.
4. R.V. Maltsev, A.K. Rebrov, Hypersonic Transversal Flow of Rarefied Gas Mixture past Infinite Band, in Proc. of 24 Intern. Symp. on RGD, AIP Conference Proceedings, 2005, Vol. 762, pp. 1229-1234
5. M. Yu. Plotnikov, A.K. Rebrov, Direct Monte Carlo Simulation of the Transverse Hypersonic Rarefied Gas Flow past a Cylinder, in Proc. of 24 Intern. Symp. on RGD, AIP Conference Proceedings, 2005, Vol. 762, pp. 1259-1264
6. Bird G. A., Molecular Gas Dynamics and the Direct Simulation of Gas Flows. Oxford: Clarendon Press, 1994
7. Plotnikov M. Yu., Fluid Dynamics. 2004. Vol. 39, N 3, p. 495-502.